Marine Pollution Bulletin, Vol. 51, No. 8-12, 2005, pp. 1078-1084

An Unsteady Three-Dimensional Eutrophication Model in Tolo Harbour, Hong Kong

K.W. Chau
Department of Civil & Structural Engineering, Hong Kong Polytechnic University, Hunghom, Kowloon, Hong Kong.

Abstract
The eutrophication phenomenon often leads to undesirable water quality. This paper delineates an unsteady three-dimensional finite difference numerical model for eutrophication dynamics in the coastal waters of Tolo Harbour, Hong Kong, employing the numerically generated, boundary-fitted, orthogonal curvilinear grid system as well as a grid "block" technique. It models the transport and interaction of nine water quality constituents. Adjustments of values of some kinetic coefficients in the model are effected through calibration with field data. It is demonstrated that the model can reasonably reproduce the interactions amongst all the water quality constituents, the eutrophication processes and, in particular, the featured bottom water anoxic condition during the summer in Tolo Harbour.

Keywords: Eutrophication; hydrodynamic modeling; unsteady modeling; Tolo Harbour; water quality modeling

Introduction

During the past, many areas of the coastal waters of Hong Kong received sewage directly from the urbanized catchments, which conveyed a heavy load of nutrients and resulted in high eutrophic potential and deterioration of water quality. Coupled with the rapid growth in economic development, the increasing tendency of eutrophication phenomena in Tolo Harbour is evidenced by a drastic increase in the severity and frequency of algae blooms (EPDHK, 2003). Various problems, including undesirable water quality, bottom-water anoxia, decline in fisheries, and loss of submerged aquatic vegetation, etc., have resulted (Hodgkiss and Chan, 1983; Sin and Chau, 1992; Chau *et al.*, 1996).

Previous research on eutrophication was focussed on seasonal steady-state conditions and then time-varied modeling with a few water quality state variables (Orlob, 1983; Lung *et al.*, 1993). A hydrodynamic model and eutrophication model have been coupled together for the evaluation of various feasible management strategies to accomplish the long-term recovery of an ecosystem (Cerco and Cole, 1993). In Tolo Harbour, research has been carried out with a view to predicting

and recording the effects of development on levels of pollution in the water (Chau and Sin, 1992; Chau *et al.*, 1996; Hodgkiss and Chan, 1983; Sin and Chau, 1992). With the recent rapid advancement of computer technology, the domain problem can now be epitomized fully in an unsteady manner. Moreover, the anoxic status in bottom waters of Tolo Harbour during the summer cannot be simulated satisfactorily using a conventional depth-integrated model, rendering it necessary to develop a fully depth resolved model. In this paper, a rigorous three-dimensional (3D) numerical eutrophication model, integrating hydrodynamics with water quality and sediment nutrient release to simulate time-varying water quality transport, is presented. The prototype model has been developed, calibrated, and verified for Tolo Harbour, Hong Kong.

Existing Conditions in Tolo Harbour

Figure 1 shows a map of Tolo Harbour, with an area of about 52 square kilometres, it is an almost land-locked body of water with a narrow outlet into the South China Sea. The average water depth is 12m, with an average diurnal tidal difference of 0.97 m. The water in the inner harbour has been seriously polluted due to substantial pollution loads and poor tidal flushing. The differences in surface and bottom water temperature and salinity result in density stratification within the water column during the summer (Chau and Jin, 1995), which weakens vertical mixing. Bottom waters in Tolo Harbour exhibit serious dissolved oxygen (DO) depletion whilst the DO content remains adequate at the surface (EPDHK, 2003). The harbour is classified as highly eutrophic, shown by its high algal growth. However, in winter, owing to lower bottom sediment oxygen demand (SOD) exerted at lower temperatures as well as an increase of turbulent mixing due to the strong northeast monsoon, higher DO levels in the bottom waters are attained.

Formulation of Model

Three organic state variables (carbonaceous biochemical oxygen demand (CBOD), nitrogen and phosphorus (including both dissolved organic matter and particulate organic matter for nitrogen and phosphorus)), four inorganic state variables (DO, ammonia (NH_4), nitrite and nitrate ($NO_2 + NO_3$), and orthophosphate (PO_4)), and two biological constituents (phytoplankton and zooplankton) were taken into consideration in the formulation of this model. Organic nitrogen, organic phosphorus, and PO_4 exist under two different phases, namely, particulate and dissolved (Ambrose *et al.*, 1988; Lung, 1993)). Only the dissolved phase is available for phytoplankton uptake. The existing 10 years' field data collected during the period of 1993-2002 in Tolo Harbour showed that silicate is plentiful and is excluded as a limiting nutrient. Hourly data of solar radiation intensity, water temperature, and salinity are also used (EPDHK, 2003).

The coupled model is tailored to have a common computational grid and time steps for both the hydrodynamic and water quality processes. In the following sections, subscript "k", "u" and "l" represent the value in the k^{th} layer, upper layer, and lower layer, respectively. The following differential transport equations are expressed for layer-averaged concentration of an individual state variable under the boundary-fitted orthogonal curvilinear co-ordinate system (Thompson *et al.*, 1985; Chau and Jiang, 2002):

$$\frac{\partial(h_k\varphi_k)}{\partial t}+\frac{1}{g_{11}g_{22}}\left\{\frac{\partial}{\partial\xi}\left[g_{22}h_k\left(u_k^*\varphi_k-\frac{\Gamma_{\xi,k}}{g_{11}}\frac{\varphi_k}{\partial\xi}\right)\right]+\frac{\partial}{\partial\eta}\left[g_{11}h_k\left(v_k^*\varphi_k-\frac{\Gamma_{\eta,k}}{g_{22}}\frac{\varphi_k}{\partial\eta}\right)\right]\right\}=\Phi_{\varphi,k} \quad (1)$$

$$\Phi_{\varphi,k}=w_k\varphi_k+Flux_{u,\varphi}-Flux_{l,\varphi}+S_{\varphi,k} \quad (2)$$

where u_k^* and v_k^* = layer-averaged velocity components in ξ-η orthogonal curvilinear co-ordinates; h_k = water depth; φ_k = layer-averaged concentration of the state variable, representing DO, phytoplankton, or other water quality state variables; $\Gamma_{\xi,\kappa}$ and $\Gamma_{\eta,\kappa}$ = longitudinal and transverse dispersive coefficients, respectively: g_{11} and g_{22} = co-ordinate transformation coefficients between Cartesian and orthogonal curvilinear co-ordinates (ξ,η); $S_{\varphi,k}$ = reaction kinetics, settling, sediment release, sources, or sinks and w_k = vertical velocity at the layer interface (Rodi, 1980; Fischer *et al.*, 1979).

A staggered grid (Arakawa C) system is adopted, in which the nodes for water quality state variables and water surface elevation do not coincide with those of water velocities (Chau and Jin, 1995). The set of differential transport equations is then discretized by control-volume formulation, expressing the conservation principle for the variable. The computational domain is divided into non-overlapping control volumes surrounding every grid point. The equation is integrated over each control volume with piecewise profiles expressing the variation of the variable between the grid points (Yih, 1980). After integrating Eq. 1 in the control volume, an equation set of discretized equations for each state variable can be solved by a tri-diagonal matrix algorithm with alternating direction iteration (Patankar, 1980). The procedure of the solution in one time step calculates the hydrodynaimc variables first and then those for phytoplankton, zooplankton, organic nitrogen, NH_4, NO_2+NO_3, organic phosphorus, PO_4, CBOD and DO in turn.

The following processes, as depicted in Figure 2, are simulated in the model. Settlement reduces quantities of water quality variables whilst the rate of algal growth is related to available nutrients, water temperature, solar radiation, zooplankton grazing, and tidal flushing. Organic nitrogen undergoes a bacterial decomposition with ammonia (NH_4) as the end product. Organic

phosphorus is converted to PO_4 by mineralization. Ammonia nitrogen, in the presence of nitrifying bacteria and oxygen, is converted to NO_3-N. Denitrification occurs under anaerobic conditions and CBOD decreases due to stabilization. Whilst both NH_4 and $NO_2 + NO_3$ are available for algae uptake, the preferred form is NH_4 for physiological reasons. The production of DO is a by-product of photosynthetic carbon fixation. An additional source of oxygen from algal growth occurs when the available ammonia nutrient source is exhausted and the phytoplankton begins to utilize the available nitrate. The initial step for nitrate uptake is the reduction to ammonia with the production of oxygen. Owing to the deficit from the saturation concentration, DO increases by atmospheric re-aeration, with a rate dependent on internal mixing and turbulence due to velocity gradients and fluctuation, temperature, wind mixing, waterfalls, dams, rapids, surface films, etc. An adsorption-desorption interaction exists between dissolved inorganic phosphorus and suspended particulate matter in the water column. The settling of the suspended solids and the inorganic phosphorus becomes a source of phosphorus for the sediment (Orlob, 1983; Lung, 1993).

Various kinetic reaction coefficients are calibrated with the field data or come from the literature (Thomann and Mueller, 1987; Ambrose *et al.*, 1988). During the photosynthesis process, the growth rate of phytoplankton depends highly on temperature, solar radiation, and nutrients. The light-limitation function of Steele and Baird (Thomann and Mueller, 1987; Lung, 1993), with measured hourly daily solar radiation intensity supplied by the Royal Observatory of Hong Kong, is employed here. The minimum value of nutrient limitations computed with the Michaelis-Menten-type expression (Thomann and Mueller, 1987; Lung, 1993) is adopted. Apart from these factors, the C:Chl ratio (mg C/mg Chl-a) also depends highly upon the past history of the algal cells (Jin *et al.*, 1998).

A saturating recycle equation is used for hydrolysis and bacterial decomposition of organic nitrogen to ammonia and the mineralization of organic phosphorus to inorganic phosphorus. This mechanism slows the recycle rate if the algal population is small but does not permit the rate to increase continuously as phytoplankton increases since at higher population levels other factors are limiting the recycle kinetics. The processes of nitrification of NH_4 to NO_3 via NO_2, denitrification of NO_3 and deoxygenation of CBOD are considered temperature and oxygen dependent (Ambrose *et al.*, 1988; Lung, 1993).

Primary production by phytoplankton in surface waters is a major source of labile organic carbon to coastal sediment. Particles from the euphotic zone sink to the sediment-water interface, where benthic organisms rapidly degrade the labile organic compounds present in the settled materials (Di Toro *et al.*, 1990). Sediment nutrient releases, as a result of a gradient in nutrient concentration between the overlying water and the nutrient in the interstitial water, can lead to

continuing eutrophication problems even after point sources are substantially reduced through control measures (Lung, 1993).

Tolo Harbour Model

In order to adapt the complicated boundaries of Tolo Harbour, a boundary-fitted orthogonal curvilinear grid system with a total of 1580 grid cells is employed. Longitudinal grid size varies between 110-710 m and transverse size between 60-530 m. A grid "block" technique (Chau and Jiang, 2001 & 2002) is employed to avoid the usual computational difficulty of unsteady fluctuation of water surface level. Tidal elevation at the open boundary is computed from a harmonic tidal analysis based on long term measurement at Kau Lau Wan using 42 tidal constituents. The normal gradients for all water quality variables at bank boundary are specified as zero. The concentrations of all water quality variables at the open boundary are specified with measured data when water flows into the water body of interest whilst the normal gradients of the concentrations are simply taken as zero when water flows out from the water body. The initial conditions are assumed by interpolating the corresponding boundary values at the starting time.

The pollution sources entering the harbour consist of those from five main tributaries and two time-varying point sources representing outfalls of two sewage treatment plants (EPDHK, 2003). According to the vertical positions of the point sources entering the waters, they are placed in the relevant layer. Around the inner harbour most of the non-point sources flow into the streams and the sewage treatment plants, and a rural mountain area exists on the two sides of the Tolo Channel. Non-point sources are scarce and are not considered in the simulation. Based on in-situ field study, the average SOD in Tolo Harbour is determined to be 0.88 g O_2/m^2/day (Chau, 2002).

Verification Results and Discussions

The verification results show that the flow directions in the surface and the bottom layers in the harbour, particularly in the side coves, may be opposite. The computed velocities in most of the harbour, especially in Tolo Channel, have a prevailing direction along the channel, and its transverse component is very small relative to its longitudinal counterpart.

Whilst the data measured from 1998 to 2000 are used to calibrate the kinetic parameters in the model, the model is verified by the data from 2000 to 2002. Fig. 3 compares and simulates Chl-a and DO with observations in the surface layer and bottom layer at different stations from 2000 to 2002. The fluctuation on model predictions for Chl-a and DO may be attributed to variations in light intensity, pollutant loadings, tidal flow, density stratification, water temperature and salinity,

etc. A sensitivity analysis, as shown in Table 1, has been performed which indicates that the fluctuations of Chl-a and DO are mainly due to nutrients from anthropogenic pollution loadings.

Moreover, the simulations appear to show an annual cycle with tidal variation. During the spring and the early summer, the water temperature rises as the solar radiation intensifies, the chlorophyll-a concentrations can attain their annual maximum and the nutrients are rapidly depleted by the algal bloom. The ammonia and orthophosphate concentrations in the bottom layer are higher than those in the surface layer due to less uptake by the phytoplankton and the sediment release. Meanwhile, the DO can maintain a super-saturated period due to photosynthesis and then rapidly decreases because of the activity of settled algal carbon as SOD and reaches its annual minimum. In June, bottom water anoxia may occur, especially in the inner harbour, and the anoxic condition may be retained for a prolonged period.

It is noted that fit of DO is in general better than that of Chl-a. It may suggest that DO is more driven by physical rather than by ecological processes. Fig. 4 compares and simulates all nine water quality state variables at station TM4 from 1998 to 2000. The normalized mean square errors and coefficients of correlation between computed and measured results, as shown in Table 2, are employed as performance indicators. The correlation coefficients are calculated for all stations and different stations are modeled with slightly different accuracy. Overall, the computational results mimic the measured data in Tolo Harbour and represent reasonably the algal growth dynamics and water quality processes.

The following refers to both the model and observation results. During the summer, serious oxygen depletion in the bottom waters, with DO levels below 5% saturation, occurs frequently. This can be attributed to the high oxygen demand from the decay of organic matter in the bottom sediment at higher summer temperatures. The respiration of benthos also consumes oxygen in the bottom water. The weak turbulent mixing and the steep temperature and salinity stratification in the water column prevent vertical mixing and replenishment of oxygen from the well aerated surface water to the bottom. In the winter, higher DO levels in the bottom waters are generally recorded. In this aspect, the computational results show correctly the anoxic condition in the bottom layers when the surface waters may still be well oxygenated during the summer whilst, during the winter, they adequately reflect vertically uniform water quality concentrations.

During the winter, owing to the lower water temperature and weaker solar radiation, lower chlorophyll-a concentrations occur. At the same time, saturated DO is caused mainly through mixing. During the spring and the early summer, water temperature rises and solar radiation intensifies, chlorophyll-a concentrations can attain their annual maximum and nutrients are rapidly depleted by the algal bloom. Ammonia and orthophosphate concentrations in the bottom

layer are higher than those in the surface layer due to less uptake by the phytoplankton as well as their release from the sediment. Meanwhile, the DO can maintain a super-saturated period due to photosynthesis and then rapidly decrease due to the activity of settled algal carbon as SOD and it reaches its annual minimum near June. Bottom water anoxia may occur, especially in the inner harbour. From autumn till December, a lower chlorophyll-a concentration is maintained so that both DO and nutrients may be restored gradually.

Conclusions

In this paper, an unsteady 3D numerical model for eutrophication is developed and implemented to simulate the transport and transformation of nine water quality constituents associated with eutrophication in the waters of Tolo Harbour, including Chl-a (phytoplankton), DO, CBOD, organic nitrogen, NH_4, $NO_2 + NO_3$, organic phosphorus, PO_4-P, and zooplankton. Through the comparison between computational results and measured data available in Tolo Harbour, it is shown that the model is able to adequately mimic the algal growth dynamics and water quality processes. It is used to demonstrate that polluting nutrients are the controlling factors and to explain the mechanism of how the anthropogenic inputs influence the ecosystem.

Acknowledgement

This project was supported by a grant from the Research Grant Committee of the University Grant Council of Hong Kong.

References

Ambrose, R. B., Wool, T. A., Connolly, J. P., and Schanz, R. W. (1988). *WASP4, a hydrodynamic and water quality model—model theory, user's manual, and programmer's guide.* U.S. Environmental Protection Agency Report, EPA/600/3-87/039.

Cerco, CF, and Cole, T (1993). "Three-Dimensional Eutrophication Model of Chesapeake Bay," *Journal of Environmental Engineering, ASCE,* Vol 119(6), pp 1006-1025

Chau, K.W. (2002). "Field measurements of SOD and sediment nutrient fluxes in a land-locked embayment in Hong Kong," *Advances in Environmental Research*, Vol. 6(2), pp. 135-142.

Chau, KW, and Jiang, YW (2001). "3D Numerical Model for Pearl River Estuary," *Journal of Hydraulic Engineering, ASCE*, Vol 127(1), pp 72-82.

Chau, KW, and Jiang, YW (2002). "Three-Dimensional Pollutant Transport Model for the Pearl River Estuary," *Water Research*, Vol 36(8), pp 2029-2039.

Chau, KW, and Jin, HS (1995). "Numerical Solution of Two-Layered, Two-Dimensional Tidal Flow in Boundary-Fitted Orthogonal Curvilinear Coordinate System," *International Journal for*

Numerical Methods in Fluids, Vol 21(11), pp 1087-1107.

Chau, KW, Jin, HS, and Sin, YS (1996). "A Finite Difference Model of 2-D Tidal Flow in Tolo Harbour, Hong Kong," *Applied Mathematical Modelling*, Vol 20(4), pp. 321-328.

Chau, KW, and Sin, YS (1992). "Correlation of Water Quality Parameters in Tolo Harbour, Hong Kong," *Water Science and Technology*, Vol 26(9-11), pp. 2555-2558.

Di Toro, DM, Paquin, PR, Subburamu, K, and Gruber, DA (1990). "Sediment Oxygen Demand Model: Methane and Ammonia Oxidation," *Journal of Environmental Engineering, ASCE,* Vol 116(5), pp 945-986.

EPDHK (2003). *Marine Water Quality in Hong Kong:Results from the EPD Marine Water Quality Monitoring Programme for 2002,* Environmental Protection Department, Hong Kong Government, EP/TR 3/00.

Fischer, H. B., List, E. J., Koh, R. C. Y., Imberger, J., and Brooks, N. H. (1979). *Mixing in Inland and Coastal Waters.* Academic Press, Inc., San Diego, Calif.

Hodgkiss, IJ, and Chan, BSS (1983). "Pollution Studies on Tolo Harbour, Hong Kong," *Marine Environmental Research,* Vol 10, pp 1-44.

Jin, Haisheng, Egashira, Shinji and Chau, K.W. (1998). "Carbon to chlorophyll-a ratio in modeling long-term eutrophication phenomena," *Water Science and Technology*, Vol. 38(11), pp. 227-235.

Lung, W.S. (1993). *Water Quality Modeling, Vol. III: Application to estuaries,* CRC Press, Inc., Boca Raton, Fla.

Lung, W., Martin, JL, and McCutcheon, SC (1993). "Eutrophication Analysis of Embayments in Prince William Sound, Alaska," *Journal of Environmental Engineering, ASCE,* Vol 119(5), pp 811-824.

Orlob, G. T. (1983). *Mathematical Modeling of Water Quality.* Wiley-Interscience, New York, N. Y.

Patankar, S.V. (1980). *Numerical Heat Transfer and Fluid Flow.* Hemisphere Publishing Corporation.

Rodi, W. (1980). *Turbulence Models and Their Application in Hydraulics, state-of-the-art.* IAHR Publication, DELFT, The Netherlands.

Sin, YS, and Chau, KW (1992). "Eutrophication Studies on Tolo Harbour, Hong Kong," *Water Science and Technology,* Vol 26(9-11), pp 2551-2554.

Thomann, RV, and Mueller, JA (1987). *Principles of Surface Water Quality Modeling and Control,* Harper & Row, Publishers, Inc., New York, N. Y.

Thompson, J. F., Warsi, Z. U. A., and Mastin, C.W. (1985). *Numerical grid generation*. Elsevier Science Publishing Co., Inc., New York, N. Y.

Yih, C. S. (1980). *Stratified Flows*. Academic Press.

Table 1. Sensitivity analysis of effects of different factors on the fluctuations of Chl-a and DO

20% change on constituent factor	% change	
	Chl-a	DO
Nitrogen nutrient	11.3	13.5
Phosphorus nutrient	6.1	7.2
Light intensity	2.0	2.9
Water temperature	0.7	0.5
Tidal flow velocity	0.4	0.4
Density stratification	0.1	0.1

Table 2. Normalized mean square errors (NMSE) and coefficients of correlation (CC) between the computed and measured results during calibration and verification stages

Water quality state variable	During calibration stage		During verification stage	
	NMSE	CC	NMSE	CC
Chl-a	0.631	0.833	0.645	0.812
DO	0.547	0.914	0.597	0.904
$CBOD_5$	0.589	0.924	0.602	0.897
Organic N	0.613	0.912	0.647	0.895
NH_4-N	0.621	0.934	0.658	0.887
NO_2+NO_3-N	0.625	0.910	0.667	0.858
Organic P	0.631	0.903	0.649	0.889
PO_4-P	0.622	0.915	0.639	0.874

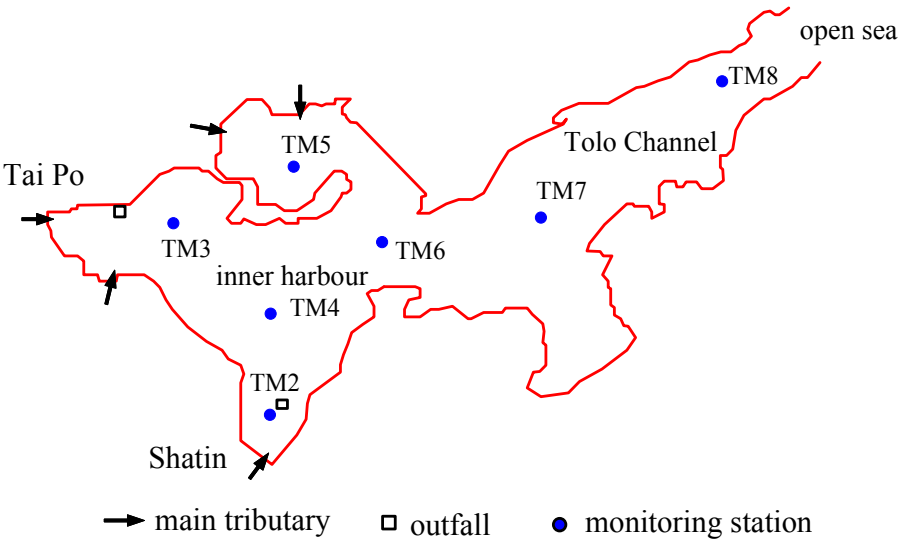

Fig.1 The Tolo Harbour, Hong Kong

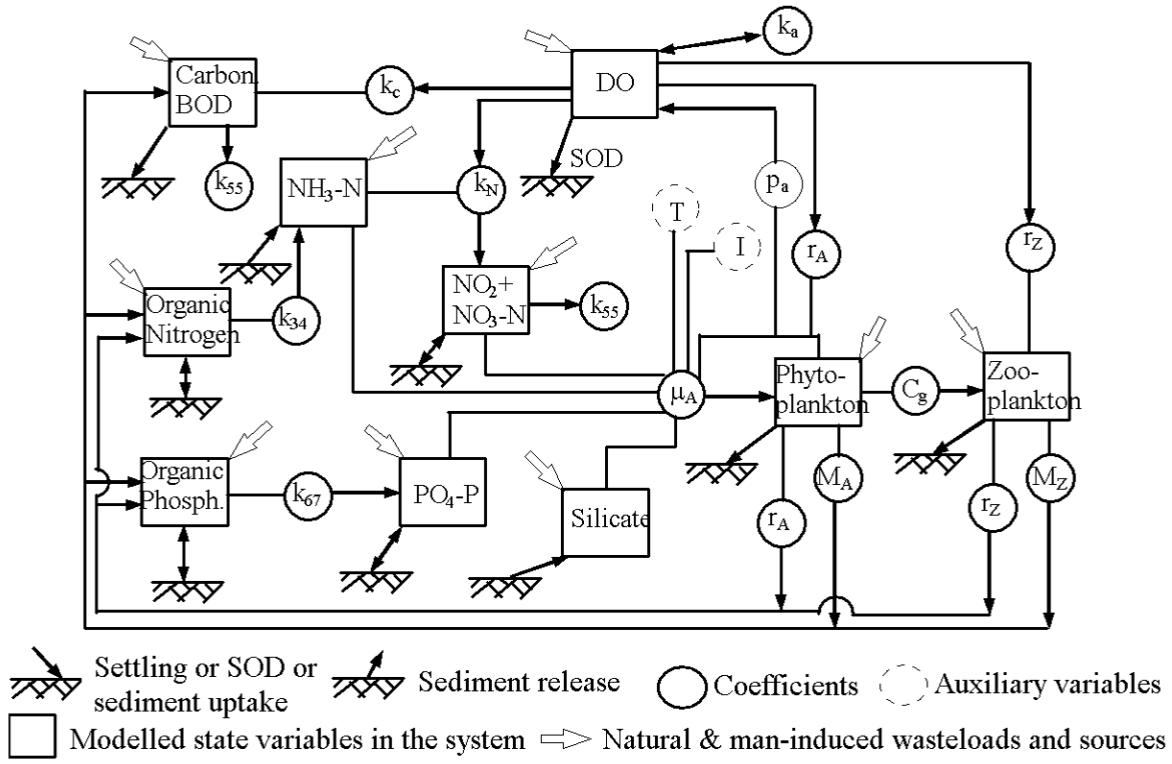

Fig. 2 Model state variables and their interactions

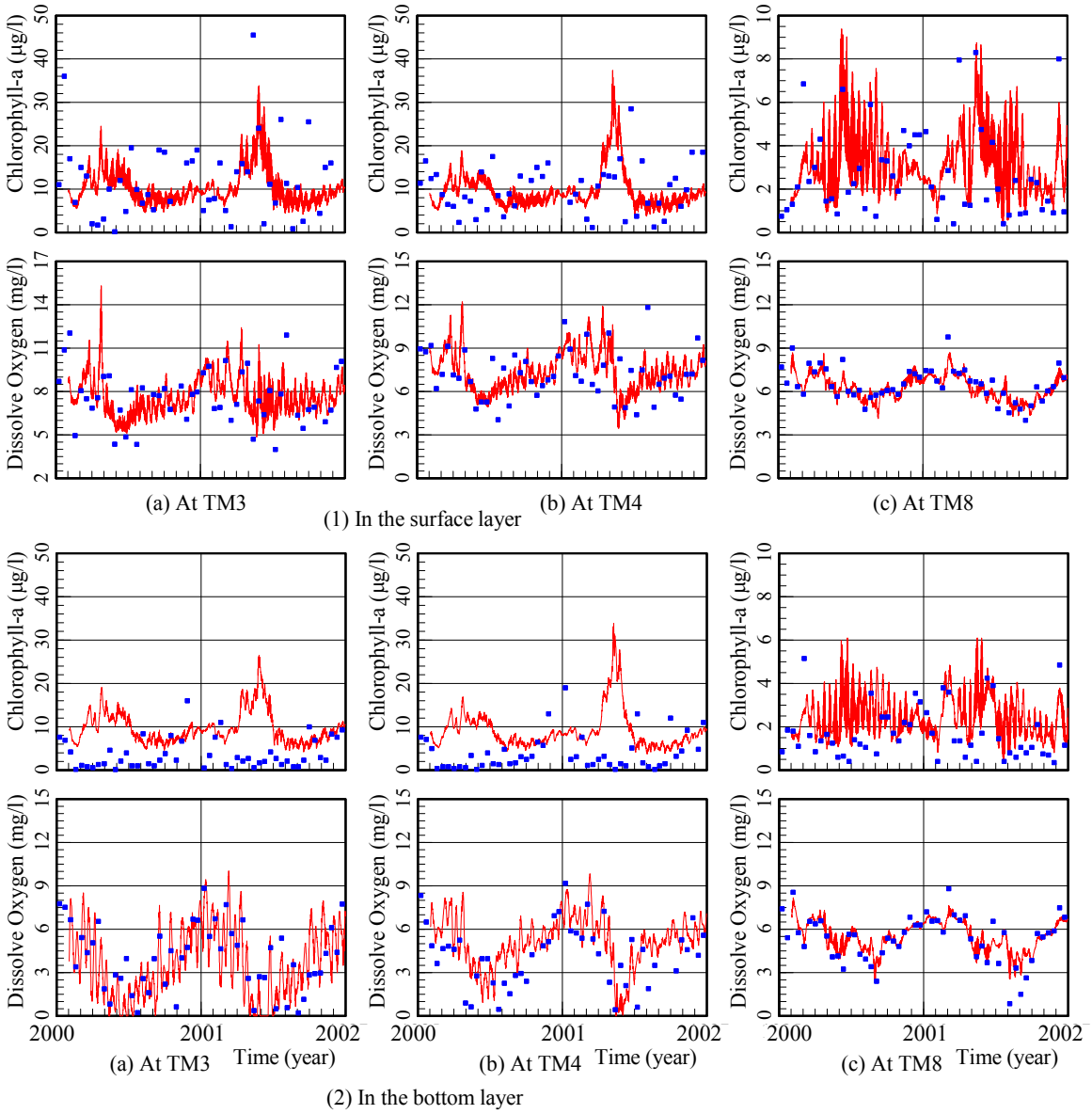

Fig.3 Computed and measured results of Chl-a and DO at different stations from years 2000 to 2002 (— computed, ▪ measured)

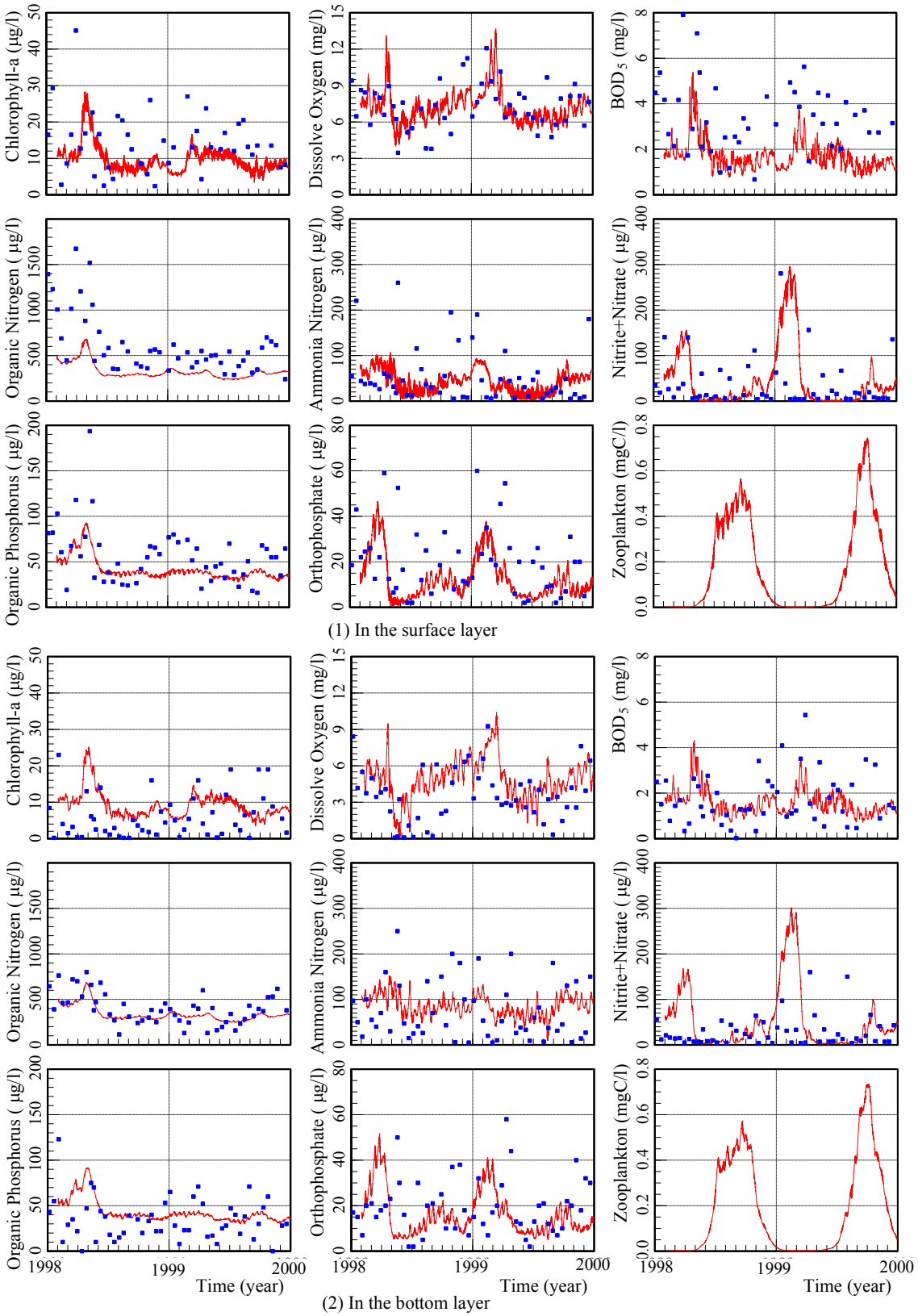

Fig.4 Comparisons of results computed and measured at TM4 from years 1998 to 2000 (— computed, ▪ measured)